

Structural and optical properties of Si-doped GaN

A. Cremades,* L. Görgens, O. Ambacher, and M. Stutzmann

Walter Schottky Institut, Technische Universität München, Am Coulombwall, D-85748 Garching, Germany

F. Scholz

Physikalisches Institut, Universität Stuttgart, Pfaffenwaldring 57, D-70550 Stuttgart, Germany

(Received 28 July 1999)

Structural and optical properties of Si-doped GaN thin films grown by metal-organic chemical vapor deposition have been studied by means of high resolution x-ray diffraction (XRD), atomic force microscopy, photoluminescence, photothermal deflection spectroscopy, and optical transmission measurements. The incorporation of silicon in the GaN films leads to pronounced tensile stress. The energy position of the neutral donor bound excitonic emission correlates with the measured stress. The stress induced near band gap luminescence shift is estimated to 19 ± 2 meV/GPa. An increasing concentration of dopant impurities in the films leads to asymmetries of the XRD and photoluminescence spectra, which are probably related to a stress induced inhomogeneous distribution of dopants. Atomic force microscopy observations of surface modulation with increasing silicon doping support this latter statement. Transmission and photothermal deflection spectroscopy measurements are used to determine the band gap energy and Urbach energy of highly doped samples.

I. INTRODUCTION

Silicon has become the usual donor in intentionally doped *n*-type GaN films. It has a shallow donor level with an ionization energy of 30 meV.¹⁻³ The dependence of the optical, electrical, and structural properties of the GaN thin films on Si doping has already been reported,⁴⁻⁸ although the observed trends are not well understood. Among others, the stress relaxation in Si-doped GaN and undoped GaN films has been the focus of recent studies.^{4,9-11} The effect of silicon doping on the mechanism of stress relaxation and defect formation in GaN is still under discussion. Ruvimov *et al.*⁴ suggest that the thermal stress is partly relaxed by migration of threading dislocations, leaving additional misfit dislocations in the basal plane. On the other hand, Lee *et al.*⁹ discuss a silicon-doping induced defect formation during the cool-down process as a possible origin of the stress relaxation. Results of other authors⁶ indicate that the strain relaxation due to Si incorporation is not significant up to Si concentrations of 2×10^{17} cm⁻³. Concerning the optical properties, a shift of the optical band gap E_g towards lower energies with increasing silicon doping has often been observed, which was attributed to strain relaxation.⁴ The observed strong correlation between electrical and optical properties⁴ is explained by a model which assumes a random distribution of impurities and defects that may produce local strain and potential fluctuations.^{4,8}

In the present work silicon doped GaN films grown by metal-organic chemical vapor deposition (MOCVD) have been characterized by means of highly resolved x-ray diffraction (HRXRD), atomic force microscopy (AFM), photoluminescence (PL), photothermal deflection spectroscopy (PDS), and transmission measurements in order to study in detail the effect of silicon doping on the structure and the optical properties of GaN films. Special attention is paid to the discussion of stress related effects and the shift of the band gap energy observed for strong Si doping.

II. EXPERIMENT

1- μ m-thick samples have been grown by means of (MOCVD) on *c*-plane sapphire using triethylgallium (TEG) and ammonia at substrate temperatures of 1000 °C. To improve the structural properties of the films, a GaN buffer layer was grown at low temperature. The samples were transparent and mirrorlike. The carrier concentration and mobilities of the samples were determined by Hall measurements and atomic force microscopy was used to investigate the sample surface. XRD measurements have been performed with a Phillips X'Pert mrd diffractometer equipped with a PW3050120 goniometer, a channel cut Ge[220] analyzer, and a 4-crystal monochromator in Ge[220] mode. The resolution achieved is $\Delta\theta = 12''$.

PL measurements have been performed under excitation with the 351.1-nm line of an Ar⁺ laser, using an excitation power of 20 mW. A continuous flow He cryostat was used for temperature variation from 5 to 300 K. The luminescence was detected with a 0.8-m double monochromator and a cooled photomultiplier in the photon counting mode. To determine the absorption coefficient of the silicon doped layers versus energy, we have used transverse PDS^{12,13} and transmission measurements using a Perkin Elmer Lambda 900 double beam spectrometer with a resolution between 1 and 5 nm in the range 0.6–4 eV. The attractive feature of PDS is its extremely high sensitivity. Absorbance values of group-III-nitride epitaxial films on sapphire substrates as low as $\alpha d = 10^{-4}$ (α is the absorption coefficient and the d thickness) can be determined. Details concerning the use of PDS for characterization of group-III nitrides have been reported elsewhere.¹⁴

III. RESULTS

A. XRD

In Table I we summarize the carrier concentration and structural data of the samples investigated here. In order to

TABLE I. Electrical and structural parameters of the samples: carrier concentration n , lattice constants a and c , hydrostatic stress σ_{hyd} , in-plane stress σ_{\parallel} , and layer thickness d .

Sample	n (cm ⁻³)	a (Å)	c (Å)	σ_{hyd} (GPa)	σ_{\parallel} (GPa)	d (nm)
A	4.7×10^{16}	3.1815	5.1909	-0.07	-0.96	1100
B	3.0×10^{17}	3.1818	5.1906	-0.07	-0.92	920
C	1.0×10^{18}	3.1872	5.1868	-0.07	-0.16	1470
D	2.2×10^{18}	3.1898	5.1846	-0.07	0.21	2095
E	5.0×10^{18}	3.1898	5.1841	-0.07	0.22	1375
F	8.0×10^{18}	3.1917	5.1826	-0.07	0.51	1120

study the structural quality and to determine the lattice constants of the samples, $2\Theta-\Omega$ scans and rocking curves were recorded for the symmetric reflections (002), (004), and (006), as well as a reciprocal space map (RSM) for the asymmetric reflection (205). From a comparison of the FWHM of the different symmetric reflections¹⁵ the broadening of the rocking curves can be ascribed to an increasing tilt of the samples. The full width at half maximum (FWHM) of the rocking curves are about 50 arcsec for all the samples, with a minimum FWHM of 30 arcsec for the undoped sample and a maximum FWHM of 75 arcsec for the sample with the highest carrier concentration. This shows the high structural quality of the layers. The shape of the $2\Theta-\Omega$ scans shows a strong dependence on the carrier concentration, as shown in Fig. 1. The asymmetric shape of the $2\Theta-\Omega$ scan can be attributed to a stress gradient normal to the sample surface. In addition thin film oscillations are observed for the $2\Theta-\Omega$ scan of undoped GaN. These oscillations are usually not seen for a layer thickness of about $1\mu\text{m}$ and demonstrate the extremely flat surfaces and the overall high structural quality of the sample. With increasing doping level the asymmetry of the $2\Theta-\Omega$ scans grows and an additional shoulder appears on the side of greater c lattice constants. None of the doped samples show any oscillations. The lattice constants have been calculated taking the refractive index correction into account as follows:

$$d_{hkl} = (\lambda/2) \sin \Theta [1 - (1-n)/\sin^2 \Theta], \quad (1)$$

λ being the x-ray wavelength, n the corresponding refractive index of GaN, and d_{hkl} the distance between planes given by

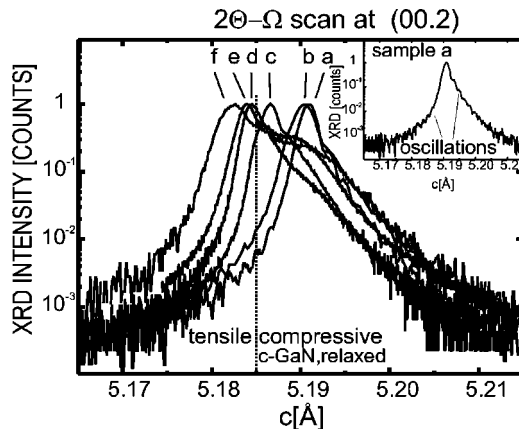


FIG. 1. $2\Theta-\Omega$ scans of the doped samples. In the inset the $2\Theta-\Omega$ scan of the undoped GaN film (sample A) is shown for illustration of the oscillations due to the changes in film thickness.

the Miller indices (hkl). The c lattice constants were calculated from all the symmetric reflections, while the a lattice constant could only be calculated from the asymmetric (205) reflex. The achieved precision was $\Delta c/c = 5 \times 10^{-5}$ and $\Delta a/a = 1 \times 10^{-4}$. In Fig. 2 the a vs c lattice constants for the samples are plotted and compared to data for fully relaxed GaN.¹⁶ The measured values follow a straight line as would be expected for biaxial stress, with the undoped and weakly doped samples under compressive stress and the higher doped samples under tensile stress. In order to understand this observation, we have calculated the change of the lattice constants for GaN and sapphire during the cool-down process. The difference of the thermal expansion coefficients (TEC) of the substrate and the epitaxial layer can account for the compressive stress found for the undoped sample.^{17,18} This leads to the conclusion that the deposited layers were fully relaxed or only slightly stressed during the growth. The incorporation of Si into the layer not only leads to strain relaxation, as generally considered, but also induces tensile strain in the layer. In addition to the biaxial strain, an overall shift towards higher lattice constants can be seen in comparison to fully relaxed GaN. This shift can be ascribed to tensile hydrostatical pressure, probably caused by point defects.

B. AFM

The AFM images of the samples show some differences depending on the carrier concentration. The AFM images of sample A, with the lowest carrier concentration of $4.7 \times 10^{16} \text{ cm}^{-3}$, and F, the one with the highest carrier concentration ($8 \times 10^{18} \text{ cm}^{-3}$), are shown in Fig. 3. Growth steps between monolayers of the crystal surface are clearly

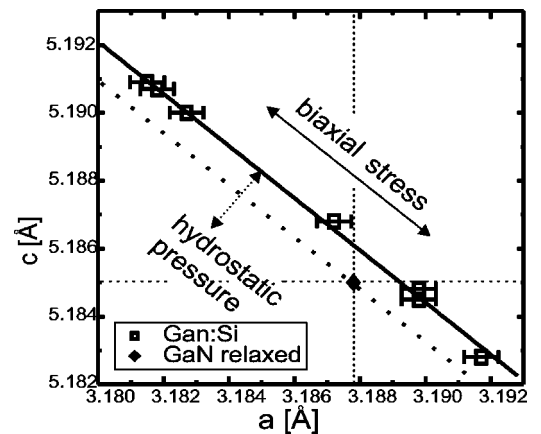


FIG. 2. Lattice constant c versus lattice constant a .

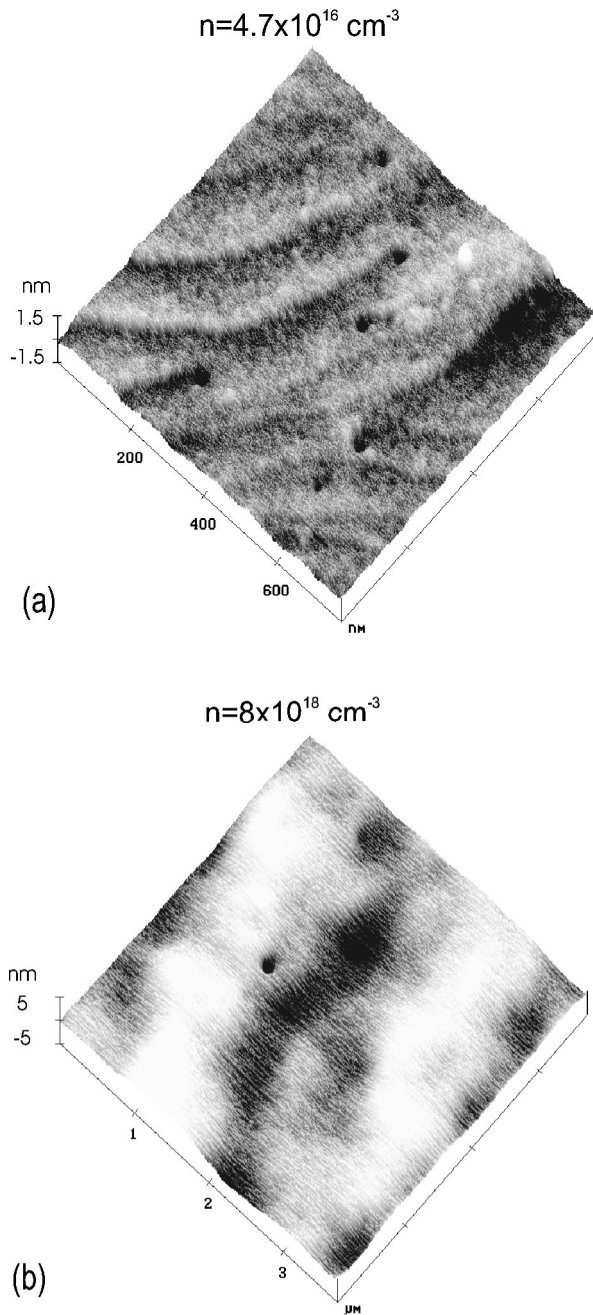
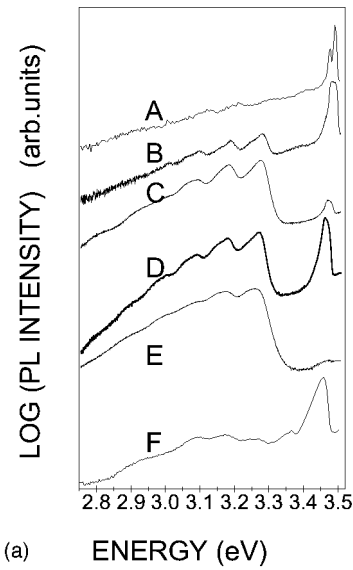
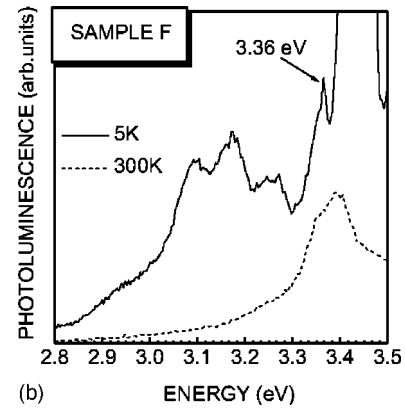


FIG. 3. AFM images of (a) undoped sample A, and (b) doped sample F.

observed for the undoped sample, together with pinholes, which seem to pin the growth steps. The surface topography is homogeneous across the sample. This surface morphology is consistent with the $2\Theta-\Omega$ scans and rocking curves for this sample showing thin film oscillations and the lowest FWHM, respectively. Sample F also has a low surface rugosity, although single growth steps are not observed. Contrary to the undoped sample, the surface of this sample shows wavelike modulations on a μm scale, with an amplitude of 8 nm. These features may be associated with local differences in the doping and/or stress distribution in the sample, which is also suggested by the asymmetric form of the corresponding $2\Theta-\Omega$ scan.



(a) ENERGY (eV)



(b) ENERGY (eV)

FIG. 4. PL spectra of (a) undoped sample A with $4.7 \times 10^{16} \text{ cm}^{-3}$ electron concentration and doped sample F with $8 \times 10^{18} \text{ cm}^{-3}$ electrons; (b) detail of the spectra of sample F recorded at low temperature and at room temperature.

C. PL

In order to study the influence of silicon doping on the radiative recombination properties of the samples, photoluminescence spectra have been recorded at different temperatures. As shown in Fig. 4(a), spectra for doped samples taken at 5 K present the well-known neutral donor bound exciton transition at about 3.45 eV for the most strongly doped sample F, together with the weak donor-acceptor pair transition with phonon replicas. The spectrum of the undoped GaN at low temperature shows two excitonic emissions at about 3.47 and 3.49 eV, which correspond to the donor bound exciton and the free exciton transitions, respectively. Again, weak donor-acceptor replicas are observed in the spectrum. In the spectrum of the most highly doped sample an additional peak of unknown nature at about 3.36 eV is observed at low temperatures, as shown in Fig. 4(b). At room temperature the donor-acceptor pair recombination is quenched, and the only observable features in the spectra, as shown in Fig. 4(b) for sample F, are near band emissions whose nature will be discussed later. The donor-acceptor pair to excitonic transition intensity ratio does not show any systematic correlation with doping. As expected, a linear relationship is ob-

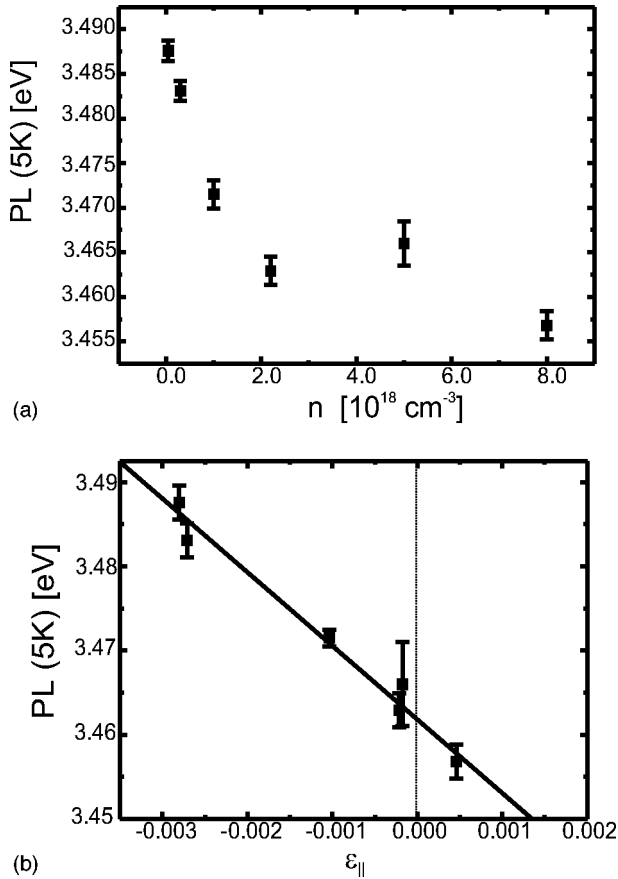


FIG. 5. Photoluminescence band gap E_g (a) versus carrier concentration and (b) versus stress.

served between the energy position of the D^0X transition and the residual in-plane-strain, ϵ_{\parallel} (Fig. 5). The slope of this linear fit has the value $k = -8.7 \pm 0.6$ eV, which is in good agreement with the data reported in the literature^{8,19} (-8.4 eV and -9.4 eV, respectively). From this fit we can estimate the position of the D^0X transition for relaxed GaN to 3.462 eV. For this estimate we have taken into account that due to the low temperature (5 K) for the PL measurements, ϵ_{\parallel} increases by 7×10^{-4} (Ref. 20) with respect to the room temperature strain measured by XRD. The position of the maximum of the band to band transition observed at room temperature exhibits also a good linear relationship with the residual in-plane strain measured by XRD. In this case the value of the slope is $k = -8.6 \pm 1.3$ eV, in agreement with the result obtained from the low temperature measurements. The D^0X transition for relaxed GaN at room temperature is estimated to 3.421 eV. A pronounced asymmetry of the excitonic transition at low as well as at room temperature is clearly observed in Fig. 4 for the strongly doped sample *F*. This result is in agreement with the asymmetry of the rocking curves. A similar asymmetry of the E_2 phonon mode in Raman measurements has been also observed.²¹ The correlation between these asymmetries observed in PL, Raman, and x-ray spectra are currently studied in more detail. Figure 6 shows the temperature dependence of the PL linewidth FWHM and the energy position of the excitonic transitions for the undoped GaN film (sample *A*) and the most strongly doped sample *F*. For the undoped sample the donor bound exciton emission disappears above 100 K.

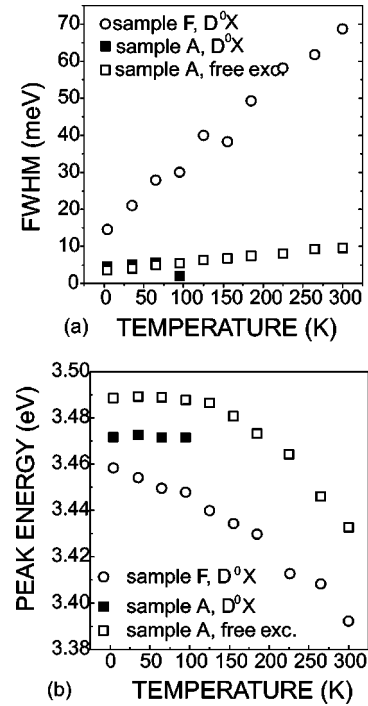


FIG. 6. Evolution with temperature of the (a) FWHM of the excitonic luminescence and (b) peak position for sample *A* ($4.7 \times 10^{16} \text{ cm}^{-3}$) and sample *F* ($8 \times 10^{18} \text{ cm}^{-3}$).

D. PDS and optical transmission

In order to determine the optical band gap E_g of the samples, transmission and PDS experiments were carried out. In Fig. 7 the PDS spectra of the samples are shown. E_g has been determined as the energy for which the absorption coefficient reaches a value of $\alpha = 10^{4.85} \text{ cm}^{-1}$.¹⁴ In undoped GaN, this value of α corresponds to the energy of the free exciton. The results are consistent with those obtained from transmission measurements. In Fig. 8(a), the values of the band gap E_g have been plotted versus the carrier concentration in the samples. For samples with carrier concentration n below $2 \times 10^{18} \text{ cm}^{-3}$ a reduction of the band gap energy is observed, while for those samples with n above $2 \times 10^{18} \text{ cm}^{-3}$ there is an increase of E_g . The contribution expected from the Burstein-Moss shift²² is also plotted. The values of the PL peak positions at 5 K and 300 K are in-

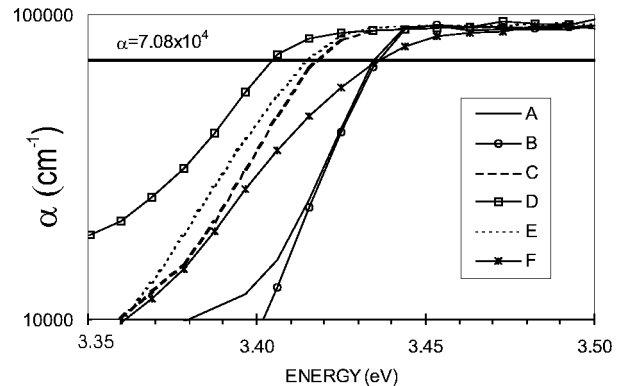


FIG. 7. Absorption coefficient of the samples calculated from the PDS spectra.

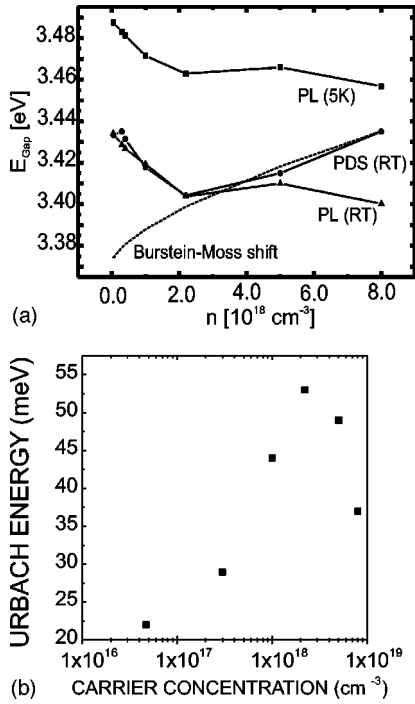


FIG. 8. (a) Comparison between the band gap energy measured by PDS and PL. The contribution of the Burstein-Moss effect is also plotted for comparison, and (b) Urbach energy vs carrier concentration in the samples.

cluded for comparison. From the exponential decay of α_{GaN} with photon energy below the band edge, an Urbach tail parameter E_{Urb} was calculated using the expression

$$\alpha = \alpha_0 \exp(\hbar\omega/E_{\text{Urb}}). \quad (2)$$

Such an exponential absorption edge can originate from structural disorder, point defects, excitonic transitions, or inhomogeneous strain in the films. The observed value of the Urbach energy versus carrier concentration is shown in Fig. 8(b).

IV. DISCUSSION

From the XRD results we conclude that the incorporation of silicon induces tensile stress in GaN films. Stress data on Si-doped GaN reported in the literature have so far been interpreted solely in terms of compressive stress relaxation because the constant of the lattice has not been measured. The origin of this relaxation is still controversial. Lee *et al.*⁹ discussed the stress relaxation as being related to Si-doping induced defects, which result in the broadening of the FWHM of the XRD reflexes. These defects would be formed during the cool-down process. This is in contradiction to the results shown by Ruvimov *et al.*⁴ They observed that the dislocation density was reduced by silicon doping. Also the c lattice constant was decreased and the bound exciton peak was shifted to lower energy. As a possible origin, Ruminov *et al.* suggested that Si mostly affects the dislocation structure during the GaN growth, perhaps by changing the atom mobility and the number of growth islands at the initial stage

of the growth, and/or changing the dislocation mobility. Aoyagi and co-workers^{23–25} have used the influence of silicon on the growth of GaN, InGaN, and AlGaN to grow quantum dots. In these studies it has been demonstrated that silicon acts as a surfactant at the initial stages of growth, inducing a three-dimensional Stranski-Krastanow growth mode.²⁶ The asymmetry of the XRD reflections is an indication of inhomogeneous stress distribution in the layer, which could also be related to an inhomogeneous distribution of dopants, as this asymmetry increases with silicon incorporation. The asymmetric peaks observed in XRD, PL, and Raman measurements may have the same origin and could be related to the surface modulation observed in the AFM images. In other material systems, as for example $\text{Ge}_x\text{Si}_{1-x}$ layers, surface ripples develop due to elastic stress relaxation, and the ripple wavelength is controlled by the germanium content.²⁷ In the same way, the surface modulation observed in our films could originate from the inhomogeneous doping induced elastic stress relaxation of the film. In addition, we have observed an increase of the FWHM of the near band PL emission with silicon doping. Such a behavior would be in agreement with the calculations based on a model of potential fluctuations caused by a random distribution of doping impurities.⁸ Band filling due to the Burstein effect²² is not taken into account as it does not play a role for $n < N_c$, where N_c is the effective conduction band density of states in GaN ($N_c = 2.3 \times 10^{18} \text{ cm}^{-3}$). Broadening due to band filling does not occur for low doping levels below N_c . Therefore the shift of the PL correlates with the residual stress ϵ_{\parallel} , as observed in Fig. 4(a). We estimate the stress induced luminescence shift to $19 \pm 2 \text{ meV/GPa}$, using the elastic constants of Ref. 28. Other values found in the literature^{11,29} for undoped GaN films are about 21–27 meV/GPa assuming biaxial compressive stress and 42 meV/GPa determined by hydrostatic pressure experiments, respectively, but depend strongly on the values used for the elastic constants. The evolution of the PL emission with temperature shows the quenching of the neutral donor bound exciton emission above 100 K for samples with low carrier concentration. In samples with high concentration of carriers there is only one excitonic emission in the whole temperature range. Based on the large energy shift between emission and absorption, emission is related to a donor bound excitons. In all cases the intensity of the excitonic emissions decays rapidly with increasing temperature showing an approximately constant integrated emission from 100 K up to room temperature. In contrast to the film with low carrier concentration, in the sample with the highest silicon doping the FWHM of the excitonic emission increases with temperature, following approximately a linear behavior from about 15 meV at 4 K to 70 meV at room temperature. This can be explained in terms of a random distribution of dopant impurities that get ionized with increasing temperature (band filling) and would be in agreement with emission due to donor bound excitons. The peak shift to lower energies with temperature is in agreement with the expected E_g shift. The comparison of the band gap energy as measured by PL and PDS, $E_g(\text{PL})$ and $E_g(\text{PDS})$ at room temperature shows good agreement for low n . This is an indication of band to band or excitonic recombination for $n \leq N_c$. In the range $n > N_c$ the emission presents a noticeable shift with respect to the ab-

sorption which increases with carrier concentration as observed in Fig. 8(a). When the carrier concentration reaches N_c band filling effects are appreciable in the absorption measurements, as absorption takes place from valence band states to free conduction band states. The formation of a silicon donor band would imply a reduction of the photoluminescence energy $E_g(\text{PL})$ with increasing carrier concentration, as illustrated in Fig. 8(a), which is in agreement with the observed Stokes shift between absorption and luminescence emission at high carrier concentrations. In addition the evolution of the Urbach energy, E_{Urb} , with carrier concentration as shown in Fig. 8(b), can be interpreted in terms of the introduction of a random distribution of dopant atoms and dopant related defects, as well as inhomogeneous stress and the formation of the silicon donor related band, in the range $n < N_c$ with increasing silicon doping. The considerable reduction of the FWHM of the rocking curves of samples with $n > N_c$ could induce the decrease of the Urbach energy. The obtained values for E_{Urb} are of the order of the equilibrium thermal disorder $kT < E_{Urb} < 2kT$ for all studied samples, which is an indication of good optical and structural quality.

V. CONCLUSIONS

Structural and optical properties of silicon-doped GaN thin films have been studied by means of XRD, AFM, PL, PDS, and transmission measurements. The silicon incorporation induced a relaxation of the compressive stress in films with low carrier density, while in films with higher concen-

tration of dopant atoms a tensile stress is observed. This is a manifestation of the strain compensation at a molecular level that takes place upon substitution of Ga atoms by silicon in the unit lattice. The most significant effect related to the silicon doping in the optical properties of the films is the stress induced shift of the excitonic emission. From our measurements the stress induced near band gap luminescence shift is estimated about 19 ± 2 meV/GPa. In films with high silicon content the neutral donor bound excitonic emission is not quenched at room temperature showing a Stokes shift to the absorption, which would be an indication of the formation or activation of a silicon-donor related band. The evolution of the optical gap E_g with temperature could be explained in terms of the stress induced optical shift, dominant for samples with a low density of carriers, and band filling, observable for samples with carrier concentration $n > N_c$, where N_c is the effective density of states in GaN ($N_c = 2.3 \times 10^{18}$ cm⁻³). The measured value of the Urbach energy is of the order of the thermally induced disorder for all studied samples, indicating good crystalline quality. Its behavior with carrier concentration may be related to the decrease of the strain dispersion in the films and the formation of a silicon donor band.

ACKNOWLEDGMENTS

This work was supported by the Bayerische Forschungstiftung (FOROPTO II). A.C. thanks the Spanish Ministerio de Educación y Cultura for a grant.

*Permanent address: Dpto. Física de Materiales, Facultad de Físicas, Universidad Complutense de Madrid, E-28040 Madrid, Spain.

¹P. Hacke, A. Maekawa, N. Koide, K. Hiramatsu, and N. Sawaki, *Jpn. J. Appl. Phys., Part 1* **33**, 6443 (1994).

²W. Götz, N.M. Johnson, C. Chen, H. Liu, C. Kuo, and W. Imler, *Appl. Phys. Lett.* **68**, 3144 (1996).

³L.B. Rowland, K. Doverspike, and D.K. Gaskill, *Appl. Phys. Lett.* **66**, 1495 (1995).

⁴S. Ruvimov, Z. Lilienthal-Weber, T. Suski, J.W. Ager III, J. Wasburn, J. Krueger, C. Kisielowski, E.R. Weber, H. Amano, and I. Akasaki, *Appl. Phys. Lett.* **69**, 990 (1996).

⁵M. Herrera Zaldívar, P. Fernández, and J. Piqueras, *J. Appl. Phys.* **83**, 462 (1998).

⁶E. Oh, H. Park, and Y. Park, *Appl. Phys. Lett.* **72**, 1848 (1998).

⁷X. Zhang, S.-J. Chuas, W. Liu, and K.-B. Chong, *Appl. Phys. Lett.* **72**, 1890 (1998).

⁸E.F. Schubert, I.D. Goepfert, W. Grieshaber, and J.M. Redwing, *Appl. Phys. Lett.* **71**, 921 (1997).

⁹I.-H. Lee, I.-H. Choi, C.R. Lee, and S.K. Noh, *Appl. Phys. Lett.* **71**, 1359 (1997).

¹⁰M. Leszczynski, T. Suski, H. Teisseyre, P. Perlin, I. Grzegory, J. Jun, S. Porowski, and T.D. Moustakas, *J. Appl. Phys.* **76**, 4909 (1994).

¹¹W. Rieger, T. Metzger, H. Angerer, R. Dimitrov, O. Ambacher, and M. Stutzmann, *Appl. Phys. Lett.* **68**, 970 (1996).

¹²A.C. Boccara, D. Fournier, W.B. Jackson, and N.M. Amer, *Opt. Lett.* **5**, 377 (1980).

¹³W.B. Jackson, N.M. Amer, A.C. Boccara, and D. Fournier, *Appl. Opt.* **20**, 1333 (1981).

¹⁴O. Ambacher, D. Brunner, R. Dimitrov, M. Stutzmann, F. Scholz, and A. Sohmer, *Jpn. J. Appl. Phys., Part 1* **37**, 745 (1998).

¹⁵T. Metzger, Dissertation, Technische Universität München, 1997.

¹⁶C. Kisielowski, J. Krüger, S. Ruvimov, T. Suski, J.W. Ager III, E. Jones, Z. Lilienthal-Weber, M. Rubin, E.R. Weber, M.D. Bremser, and R.F. Davis, *Phys. Rev. B* **54**, 17 745 (1996).

¹⁷K. Wang and R.R. Reeber, in *Nitride Semiconductors*, edited by E. Ma *et al.*, MRS Symposia Proceedings No. 482 (Materials Research Society, Pittsburgh, 1997).

¹⁸M. Leszczynski, T. Suski, H. Teisseyre, P. Perlin, I. Grzegory, J. Jun, S. Porowski, and T. Moustakas, *J. Appl. Phys.* **76**, 4909 (1994).

¹⁹V.Y. Davydov, N.S. Arerkiev, I.N. Goncharuk, D.K. Nelson, I.P. Nikitina, A.S. Polkovnikov, A.N. Smirnov, M.A. Jacobson, and O.K. Semchinova, *J. Appl. Phys.* **82**, 5097 (1997).

²⁰B.J. Skromme, H. Zhao, D. Wang, H.S. Kong, M.T. Leonard, G.E. Bulman, and R.J. Molnar, *Appl. Phys. Lett.* **71**, 829 (1997).

²¹N. Wieser (private communication).

²²E. Burstein, *Phys. Rev.* **93**, 632 (1954).

²³H. Hirayama, S. Tanaka, P. Ramvall, and Y. Aoyagi, *Appl. Phys. Lett.* **72**, 1736 (1998).

²⁴X.-Q. Shen, S. Tanaka, S. Iwai, and Y. Aoyagi, *Appl. Phys. Lett.* **72**, 344 (1998).

- ²⁵S. Tanaka, S. Iwai, and Y. Aoyagi, *Appl. Phys. Lett.* **69**, 4096 (1996).
- ²⁶I.N. Stranski and V.L. Krastanow, *Akad. Wiss. Lit. Mainz Abh. Math. Naturwiss. Kl.* **146**, 797 (1939).
- ²⁷W. Dorsch, B. Steiner, M. Albrecht, H.P. Strunk, H. Wawra, and G. Wagner, *J. Cryst. Growth* **183**, 305 (1998).
- ²⁸A.F. Wright, *J. Appl. Phys.* **82**, 2835 (1997).
- ²⁹W. Shan, J. Schmidt, R.J. Hauenstein, J.J. Song, and B. Goldenberg, *Appl. Phys. Lett.* **66**, 3492 (1995).